Figure 3(a) shows the SOA bias current dependence of the recovery time. The probe wavelength is fixed at 1550 nm and ECL output power is at 5.5 dBm. The gain recovery time changes from 45 ps to 13 ps corresponding to bias current from 200 mA to 700 mA. Afterwards the speed is limited by the resolution of our measurement setup. Figure 3(b) shows the probe wavelength dependence of gain recovery time at a constant injection current (I = 600 mA). The ECL output power is kept at 3 dBm when operated at different wavelength. With constant input powers for both the pump and probe, the gain recovery is fastest at the device gain peak and slower at the higher and lower wavelengths. This again shows that to increase the SOA gain is essential to obtain very high speed all optical operations. The proposed two-section operation makes it possible to easily obtain ~100 Gbit/s all optical devices.

1. S. Okamoto and K. Sato, in Proc. IEEE Global Telecommun. Conf., Nov. 1993, pp. 474–480.
2. Terji Durhuus *et al.*, Journal of Lightwave Technology, June 1996, Vol. 14, No. 6, pp. 942–954.
3. X. Zhao and F.S. Choa, The 1998 International Conference on Applications of Photonic Technology (ICAPT'98) Ottawa, July 27–30, 1998, Canada. Paper No. T238.

CTuK20

Wavelength dependence and cross polarization effects of nonlinear switching in an all-semiconductor-optical-amplifier loop device

Jiun-Haw Lee, Ding-An Wang, Hsin-Jiun Chiang, Ding-Wei Huang, Steffen Gurtler, C.C. Yang, Yean-Woei Kiang, *Department of Electrical Engineering and Institute of Electro-Optical Engineering, National Taiwan University, 1, Roosevelt Road, Sec. 4, Taipei, Taiwan, R.O.C.; E-mail: ccy@cc.ee.ntu.edu.tw*

We report the experimental and simulation results of the wavelength dependence and cross polarization effects of nonlinear switching in an all-semiconductor-optical-amplifier loop device. For input/output coupling, a multimode interference (MMI) amplifier was connected to the loop. The observed nonlinear switching comes from the combined effect of the nonlinear coupling in the MMI amplifier and the lateral wave field redistribution caused by the loop. This mechanism is different from that in a nonlinear optical loop mirror in which the nonlinear optical mechanism comes from the loop. Our device has a loop of 300 μm in radius, which is formed with a curved ridge-loading waveguide with a ridge width 4 μm. The loop is connected to an MMI waveguide with a length 460 or 500 μm and a ridge width 8 μm. This MMI waveguide serves the function of a coupler. Then, the input and output legs are formed with 4 μm wide waveguides. Both have the lengths of about 100 μm. The semiconductor optical amplifiers were fabricated on a four-period GaAs/AlGaAs multiple quantum well epitaxial structure. The fabrication procedures were the same as the typical processes for semiconductor lasers except the use of the UV-assisted cryo-etching technique for forming high-quality ridge-loading waveguides. For injecting different currents into different areas, we divided the electro-pad into four disconnected regions.

Figure 1 shows the experimental setup for our nonlinear switching measurements. A cw Ti:sapphire laser was used for providing the degenerate pump and signal. The coupling efficiency of laser into the device waveguide was estimated to be lower than 0.1%. A monochromator fixed at the input wavelength with a window of 2 nm was placed after the device for collecting signal power. Figure 2 shows the nonlinear switching results at different input wavelengths. We can see that at 849.6 nm, at which the electro-luminescence is the highest, the nonlinear switching is most efficient. At the other two wavelengths, a few nm lower than the maximum gain, nonlinear switching becomes less prominent. We observed the similar trend when we increased the wavelength from 849.6 nm. A larger separation of wavelength from this value led to a weaker nonlinear switching effect.

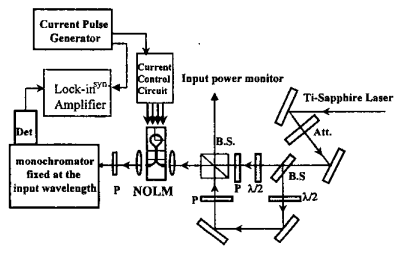

CTuK20 Fig. 1. Experimental setup for nonlinear switching measurements.

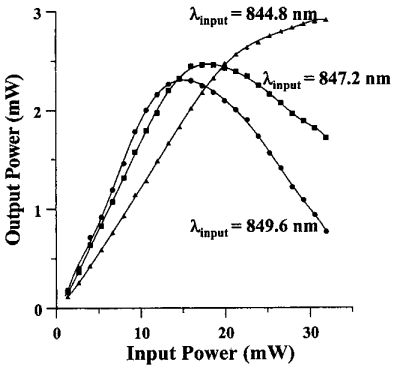

CTuK20 Fig. 2. Output power as a function of input power (the value before entering the waveguide) at different wavelengths in the TE polarization.

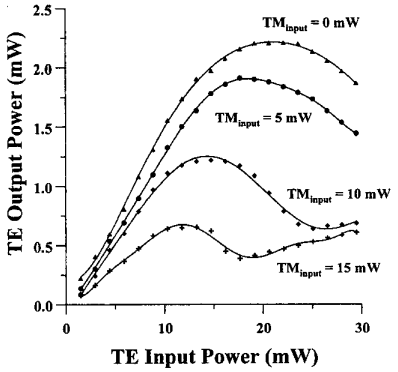

CTuK20 Fig. 3. Output power as a function of input TE signal power (the value before entering the waveguide) with different input TM signal power levels (0, 5, 10 and 15 mW for the curves from the top to bottom).

Figure 3 shows the nonlinear switching effect of the input TE signal with a cross-polarization modulation measurement. Here, the TM signal was set at 0, 5, 10 and 15 mW for the curves from the top to bottom. We can see that the input of the TM signal degrades the nonlinear switching of the TE signal. This result can be attributed to the fact that the consumption of carriers by the TM signal reduces the gain and the gain saturation effect of the TE signal. Such a phenomenon can be used for multiplexing/de-multiplexing. The nonlinear switching results with pulsed signals will also be discussed in this paper.

CTuK21

Giant optical nonlinearity and ultrafast carrier dynamics of a strained quantum well saturable Bragg reflector (SSBR)

Tze-An. Liu, Jia-min Shieh, K.F. Huang,* Ci-Ling Pan, *Institute of Electro-Optic Engineering, National Chiao Tung University, 1001 Ta-Hsueh Road, Hsinchu, Taiwan 30010; E-mail: clpan@cc.nctu.edu.tw*

Recently, semiconductor saturable Bragg reflectors (SBRs) have been successfully developed for passive mode-locking of solid state lasers.[1–3] In particular, we have developed a triple strained quantum well saturable Bragg reflector (SSBR) with saturation fluence as low as 12 μJ/cm^2.[4] This suggests potential applications of this device for applications such as all-optical swiching and modulation. In this work, we report a new type of SBR using triple strained-layer quantum wells as the absorbing layer which named strained saturated bragg reflector (SSBR). Because of it's low saturation energy and large tunning range, we want to understand the carrier dynamics with detailed wavelength. The time-resolved differention reflection (ΔR/R) in this SSBR with detailed varient pumping energies have been observed. The influence of carrier scattering and process of recombination on the temperal and spectral ΔR/R dynamics have been investigated.

The structure, reflectivity and photoluminescence spectra of the SSBR are shown in Fig. 1. Femtosecond pump/probe experiments were performed. The normalized time-resolved reflectivity, ΔR/R, of the SSBR sample as a function of the pumping wavelength are shown in Fig. 2. The wavelength-dependent peak values of ΔR/R are plotted in Fig. 3. When the sample was excited at a photon energy above the band gap ($\lambda < 757.5$ nm), ΔR/R is positive and with